



Since January 2020 Elsevier has created a COVID-19 resource centre with free information in English and Mandarin on the novel coronavirus COVID-19. The COVID-19 resource centre is hosted on Elsevier Connect, the company's public news and information website.

Elsevier hereby grants permission to make all its COVID-19-related research that is available on the COVID-19 resource centre - including this research content - immediately available in PubMed Central and other publicly funded repositories, such as the WHO COVID database with rights for unrestricted research re-use and analyses in any form or by any means with acknowledgement of the original source. These permissions are granted for free by Elsevier for as long as the COVID-19 resource centre remains active.



Comparative transcriptome analysis reveals induction of apoptosis in chicken kidney cells associated with the virulence of nephropathogenic infectious bronchitis virus



Hui Liu¹, Xin Yang¹, Zhikun Zhang, Jianan Li, Wencheng Zou, Fanya Zeng, Hongning Wang*

Key Laboratory of Bio-Resource and Eco-Environment of Ministry of Education, Animal Disease Prevention and Food Safety Key Laboratory of Sichuan Province, College of Life Sciences, Sichuan University, Chengdu 610065, Sichuan, PR China

ARTICLE INFO

Keywords:

Infectious bronchitis virus
Different virulence
Transcriptome
Kidney cells

ABSTRACT

Avian infectious bronchitis virus (IBV) that causes respiratory and nephritic diseases in chicken is a major poultry pathogen leading to serious economic loss worldwide. The nephropathogenic IBV strains cause nephritis and kidney lesions intrinsically and the pathogenic mechanism is still unclear. In the present study, SPF chicks were infected with three nephropathogenic IBVs of different virulence and their gene expression profiles in chicken kidney were compared at transcriptome level. As a result, 1279 differentially expressed (DE) genes were found in very virulent SCDY2 inoculated group, 145 in virulent SCK2 group and 74 in non-virulent LDT3-A group when compared to mock infected group. Gene Ontology (GO) and KEGG pathway enrichment analysis on SCDY2 group displayed that the up-regulated DE genes were mainly involved in cell apoptosis, and the down-regulated genes were involved in metabolic processes and DNA replication. Protein-Protein Interaction (PPI) analysis showed that DE genes in SCDY2 group formed a network, and the core of the network was composed by cell apoptosis and immune response proteins. The clustering of gene expression profile among the three virus inoculated groups indicated that the majority of up-regulated DE genes on apoptosis in very virulent SCDY2 group were up-regulated more or less in virulent SCK2 group and those down-regulated on innate immune response in SCDY2 group were also down-regulated differently in SCK2 group. In addition, the number of apoptotic cells detected experimentally in kidney tissue were very different among the three virus inoculated groups and were positively accordant with the viral titer, kidney lesions and viral virulence of each group. Taken all together, the present study revealed that virulent nephropathogenic IBV infection modified a number of gene expression and induction of apoptosis in kidney cells may be a major pathogenic determinant for virulent nephropathogenic IBV.

1. Introduction

Avian infectious bronchitis is one of the economically important virus diseases to poultry industry worldwide [1] and caused by infectious bronchitis virus (IBV), a positive-sense single-stranded RNA virus belonged to genus *Gammacoronavirus* [2–4]. The virus replicates at many epithelial surfaces of the chicken. IBV initially infects the upper respiratory tract and then spreads to kidney and oviduct, causing respiratory disease, nephritis and egg drop according the strain of the virus and the system involved [5–7]. The IBV genome is variable and variants of different genotypes have been reported worldwide [8]. Numerous serotypes and poor cross protection make it hard to control IBV spread completely in the commercial chicken farms [9–11].

The pathogenesis of IBV is complicated. In clinical case, infection of IBV is commonly followed by secondary bacterial/virus infections, which is the main cause of death and severe lesions [12]. Under the experimental conditions, the dynamic distributions of H120, M41 (respiratory type) and SAIBK (nephropathogenic) were described. They exhibited similar titers in lung, however titer of SAIBK in kidney was higher than H120, M41 at 4–10 days of post infection (dpi) [13]. Virus loads in kidney at early stage of infection may be responsible for interstitial nephritis and tubule lesions. In addition, using two dimensional gel electrophoresis, the differentially expressed proteins after infection with IBV strains were mainly relate to cytoskeleton, binding of calcium ions, the stress response, anti-oxidative and macromolecular metabolism [14].

* Corresponding author.

E-mail address: whongning@163.com (H. Wang).

¹ Hui Liu and Xin Yang have contributed equally to this work.

In order to understand the host cellular genes involved in the pathogenesis of IBV, high throughput techniques such as microarray [15–17] and RNA sequencing [18–20] were carried out. The immune responses to IBV were analyzed and a diversity of innate immunity and helper T-cell-type-1-biased adaptive immunity were activated in the host cell during early defense against IBV. Several immune factors were involved to active mucosal immunity, including toll-like receptors, type 1 interferon, interleukin 1 beta, complement, T-cell signaling molecules, surface markers and effector molecules [21]. The differential expression (DE) genes in chicken kidney after infection of ck/CH/LDL/091022 were also analyzed, 1777 DE genes were detected, including focal adhesion pathway, cytokine receptor interaction pathway, production of cell adhesion molecules and peroxisome function [15]. In addition, the DE genes in the lung tissues of IBV infected 18-days-old chicken and DE genes in the spleen of two chicken lines L10H and L10L were analyzed [16,22]. These studies exhibited a view of the molecular antiviral mechanisms of chicken response to the IBV infection. However, only one strain was used in these two reported experiments, it is difficult to compare the transcriptomics of these two strains under different animal experiments.

The infection of coronavirus has been reported with many functional and morphological changes in host cells that associated with significant changes in the patterns of expression of host cell genes [23]. Such as described in SARS-CoV [24] and mouse hepatitis virus (MHV) [25]. These results provided invaluable information on the cellular signaling pathways involved either in the cellular response to viral infections, or the viral manipulation of cellular machinery to ensure their own survival. Previous studies demonstrated that IBV could induce apoptosis in cultured cells, which may be related to the virus pathogenicity [26–28]. Only few recent studies have investigated the changes in the expression of cellular proteins during IBV infection in *ex vivo* or *in ovo* [29–31]. However, *in vivo* infection model could yield more biologically relevant insights into pathogenesis.

The present study aims to investigate gene expression profile in chicken kidney cells infected with nephropathogenic IBVs of different virulence. The comparative transcriptome analysis reveals that the interaction between virulent virus and chicken host cells might activate cell apoptosis and in turn resulted in kidney lesions.

2. Materials and methods

2.1. Viruses, animal experiment and sample collection

IBV viruses, SCDY2, SCK2 and LDT3-A, used in the study were nephropathogenic and maintained in SPF chicken embryo eggs in the laboratory of Animal Disease Prevention and Food Safety Key Laboratory of Sichuan Province. SCDY2 [32] and SCK2 [8] are very virulent and virulent nephropathogenic IBV strains respectively, isolated from Sichuan province, China. LDT3-A is an approved vaccine strain attenuated from highly nephropathogenic IBV tl/CH/LDT3/03 isolated in north China [33].

Forty white leghorn chicks hatched from SPF eggs (MERIAL-Beijing) were equally divided into four groups. At 15 days old, chicks in the three experimental groups were inoculated intranasally with 0.1 mL 10^5 , 10^5 and $10^{3.5}$ median embryo infectious doses of SCDY2, SCK2 and LDT3-A, respectively. The same volume of phosphate buffer saline (PBS) were applied to each chick in the mock inoculated control group. The chicks were then housed in separate isolators.

Chicks inoculated SCDY2 showed clinical signs at 2 dpi and three chicks died at 5 dpi and one died at 6 dpi. The gross lesions were observed in kidney with swelling and uric acid salt deposits during autopsy of the died chicks. Chicks inoculated SCK2 showed typical symptoms and slightly kidney swelling was observed at 6 dpi. No clinical signs and kidney lesions were observed in the chicks inoculated LDT3-A or PBS.

Kidney tissues were taken from the four died chicks in SCDY2

inoculated group at 5 and 6 dpi and kidney samples were also collected in parallel from the killed chicks in SCK2 or LDT3-A inoculated and mock-inoculated groups. All samples were stored at -80°C . The collection of tissue samples was performed in accordance with the Guidelines for Experimental Animals issued by the Ministry of Science and Technology of People's Republic of China.

2.2. RNA extraction, RNA sequencing and data analysis

Total RNA was isolated from collected kidney tissue with TRIzol reagent (Invitrogen, USA) following the manufacturer instructions. After quantification and qualification of the RNA samples, 3 μg RNA from each of three individuals per group at 5 dpi were mixed equally to form the input material for RNA sequencing. Libraries for RNA-seq were generated by using RNA Library Prep Kit for Illumina® (NEB, USA) and sequenced by paired-end reading on an Illumina HiSeq 4000 platform.

About 7.6 ± 1.31 G clean bases per sample were obtained and the clean reads were mapped to the genome *Gallus gallus* (http://ftp.ensembl.org/pub/release-76/fasta/gallus_gallus/dna/) with TopHat2. HTSeq v0.6.1 was used to count the number of reads mapped to each gene and FPKM (expected number of fragments per kilobase of transcript sequence per millions base pairs sequenced) of each gene was calculated based on the length of gene and the counts of paired-end reads mapped to the gene.

2.3. Analysis of DE genes

Gene differential expression analysis was carried out by using DESeq R package (1.18.0). Genes with an adjusted $\text{padj} < 0.005$ and Fold change ≥ 2 found by DESeq were assigned as DE genes. Gene Ontology (GO) enrichment of DE genes was analyzed by using of Goseq R package. The GO terms with P-value less than 0.05 were considered as significantly enriched. The enrichment of DE genes in KEGG pathways was analyzed with software KOBAS (2.0). Protein-protein interaction (PPI) of DE genes was constructed by inputting of DE genes involved in immune response, cytokine mediated signaling pathways, inflammatory response, apoptosis and cell cycling into STRING database on line (<http://string-db.org/>) and the PPI networks were visualized in cytoscape software. Clustering analysis of DE gene expression was carried out by hierarchical clustering based on FPKM of DE genes in three viruses inoculated and one mock inoculated groups. The clustered DE genes were further performed GO enrichment analysis to find out the genes related to immune response and apoptosis distributed in each cluster.

2.4. Validation of RNA-seq data and viral copies with RT-qPCR

To validate gene expression data created by RNA-seq, nine randomly selected genes with two apoptosis regulatory genes, Bax and Bcl2, were applied to reverse transcription quantitative PCR (RT-qPCR). Total RNA extracted from the same tissues as used in RNA-seq was reverse transcribed by PrimerScript™ RT Reagent Kit (Takara). Primers for amplification of these genes were listed in Table S1 and the gene expression level was estimated by $2^{-\Delta\Delta\text{CT}}$ method based on relative expression to the reference gene, β -actin. The same strategy was used to validate viral RNA copies in kidney cells by amplification of IBV 5'-UTR (Table S1) as described previously [13].

2.5. Detection of apoptosis in kidney cells by TUNEL assay

Apoptotic cells were detected by the TUNEL assay using the FITC *in situ* cell death detection kit (Roche Diagnostics, USA) according to the manufacturer's instructions. Six sections of kidney tissue for each group were stained and the results were recorded by taking pictures under fluorescence microscope (40X). The ratio of apoptotic cells for each group were determined by counting of the apoptotic cells emitting

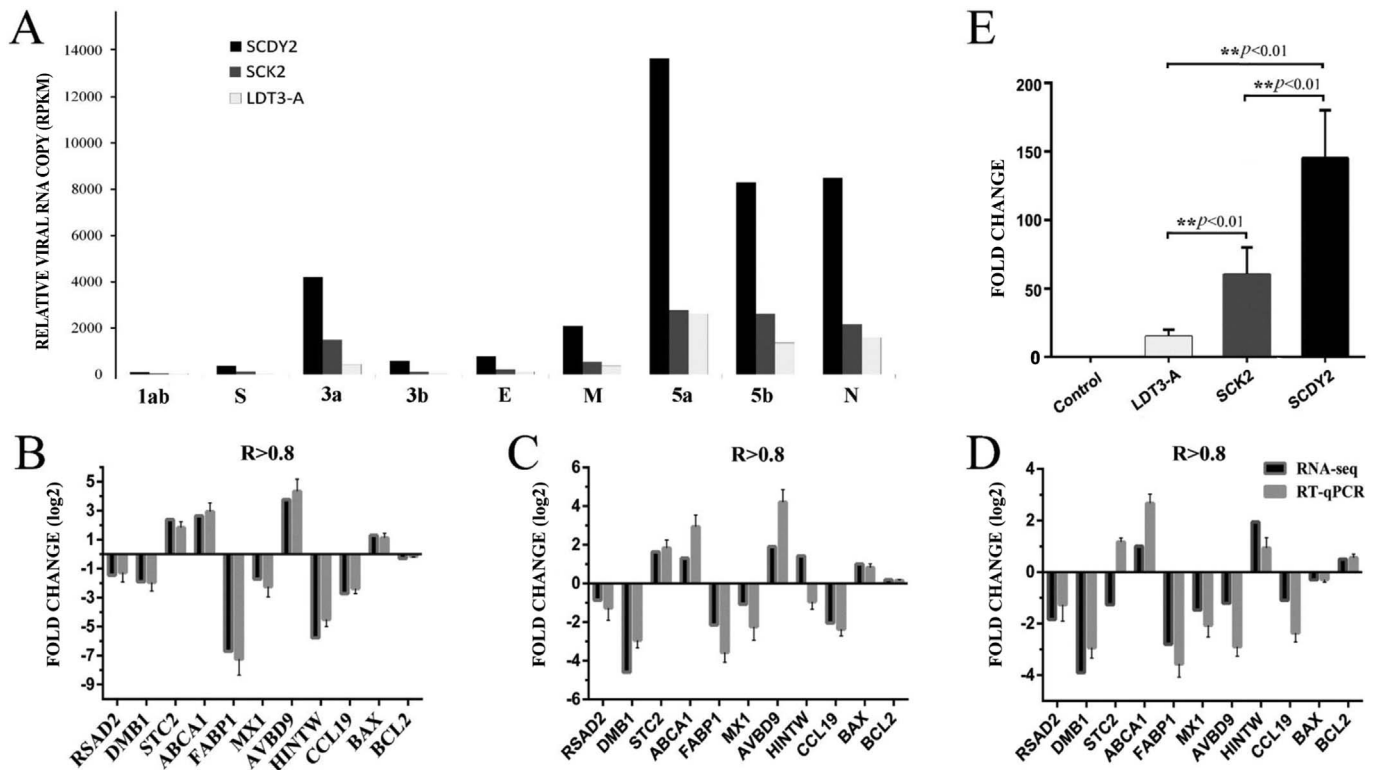


Fig. 1. Validation of viral load (A, E) and gene expression (B–D) in kidney cells post virus inoculation. Viral loads of each virus inoculated group were estimated by counting either the reads of RNA-seq mapped to each gene of viral genome (A) or the copies of viral genome in kidney cells relative to the reference gene, β -actin, through RT-qPCR (E). Reads Per Kilobase per Millions of mapped base (RPKM) was used to count the relative viral RNA copies quantitatively. The expression of selected genes in SCDY2 (B), SCK2 (C) and LDT3-A (D) inoculated groups was determined by RT-qPCR and Spearman's correlation coefficient (R) was calculated to quantify the consistency of gene expression measured by RNA-seq and RT-qPCR.

green fluorescence in at least total 2000 cells. Data are expressed as the mean \pm standard deviation.

3. Results

3.1. Data assessment and validation

About 50 million paired-end clean reads with a length of 125–150 bp were generated from RNA-seq libraries for each experimental group (mean \pm SD = 50,609,898 \pm 8,735,555) and overall 74 \pm 1.08% of the reads mapped to 14,354 \pm 125.6 genes in the reference genome of *Gallus gallus*. Some reads were aligned to viral genome. The number of reads mapped to each of the three viral genomes were variable and roughly consistent positively with the virulence of virus inoculated, e.g. the highest for very virulent strain SCDY2 and the lowest for vaccine strain LDT2-A (Fig. 1A).

To validate gene expression from the data of RNA-seq, nine genes were selected for estimation of their expression level by RT-qPCR. The consistent expression of the 9 genes between RNA-seq and RT-qPCR were analyzed by calculating of the Spearman's correlation coefficient and a significant ($R > 0.8$) correlation in each of the three virus inoculated groups were detected (Fig. 1B–D). Viral copies in the renal cells of each virus inoculated groups were also validated by RT-qPCR. Viral loads in the three experimental groups were significantly ($p < 0.01$) different, the highest detected in the SCDY2 inoculated and the lowest detected in the LDT3-A inoculated (Fig. 1E), in a trend similar as the ones detected by RNA-seq in Fig. 1A.

3.2. Functional analysis of DE genes

DE genes were analyzed by comparing of gene expression level between the infected and mock infected groups. In the group of very

virulent SCDY2 inoculated, 1279 DE genes were identified in kidney transcriptome, of which 448 were up-regulated and 831 down-regulated. However, only 145 and 74 DE genes were identified in the groups inoculated with virulent SCK2 and vaccine strain LDT3-A, respectively. In addition, the common DE genes were less among the three virus inoculated groups and more than half of DE genes (81/145) in SCK2 inoculated group were also differentially expressed in SCDY2 inoculated group, indicating regulations of gene expression among the three virus inoculated groups were different and the modification of gene expression in virulent SCK2 inoculated chicks was more similar with that in the very virulent SCDY2 inoculated, although gene expression profiles of the latter were quite different from the other two virus inoculated groups (Fig. 2).

To characterize the DE genes based on its function in each group, GO enrichment analysis was carried out and the top 30 enriched GO terms in SCDY2 group were displayed in Fig. 3. The majority of DE genes in each GO category were down-regulated and the significant enriched GO category was oxidation-reduction process. In addition, the relative up-regulation of GO (up-regulated DE genes/total DE genes enriched in the GO category) among all the 30 GO categories were cell death, apoptotic process and programmed cell death. These data indicated that activation of apoptosis and metabolic stress occurred in SCDY2 inoculated kidney cells at 5 dpi (Fig. 3).

The DE genes were further analyzed for their enrichment in KEGG pathways and results showed that in SCDY2 inoculated group the down-regulated pathways were mainly involved in metabolic pathways such as metabolism of amino acids, organic acids and other substances and DNA replication. The up-regulated pathways were oxidative phosphorylation, ABC transporters, FoxO and Jak-STAT signaling pathways (Table S2). The DE genes in SCK2 inoculated group were relative less and the enriched pathways with low rich factor were statistical meaningless.

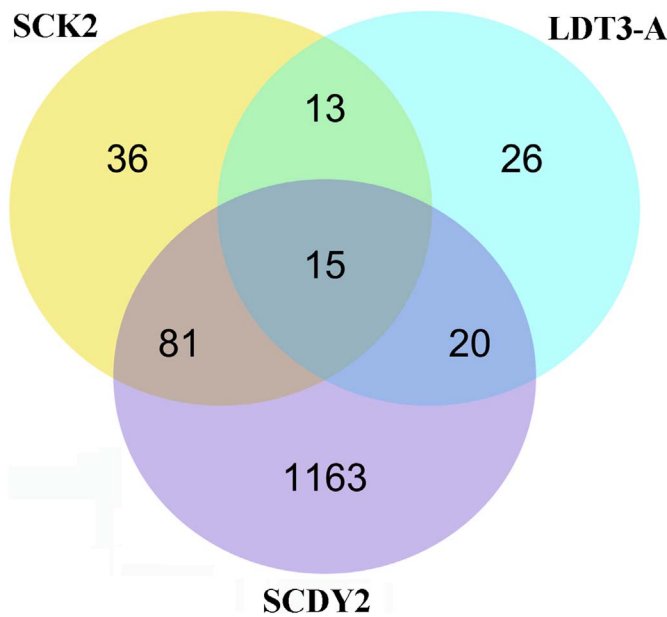


Fig. 2. Venn diagram of differential expression genes in kidney cells infected with SCDY2, SCK2 and LDT3-A of IBV virus.

Total 206 DE genes from SCDY2 inoculated group were input for STRING analysis and a predicted PPI network was built. There were two main clusters in the STRING diagram covering 74.8% of the input genes and 87.25% interactions of the network (Fig. 4). The apoptotic cluster contained 91 nodes associated with 1382 interactions (edges) and the

core nodes were BCL2L1, GADD45 and STAT3, involved in the intrinsic and extrinsic apoptotic pathways. The other small cluster with 63 nodes and 466 edges contained the core nodes of TLR3, MYD88, FADD and PIK3CG in the TLR3 pathway of innate immune response.

3.3. Clustering analysis of DE genes among different virus inoculated groups

A clustered heatmap of gene expression was built by hierarchical clustering of DE genes among the four experiment groups and the whole heatmap were classified into five parts according to gene expression patterns. Gene expression in part 1–3 generally decreased as the virulence of inoculated viruses enhanced, and the roughly reversed gene expression profiles were exhibited in part 4–5 (Fig. 5A). To estimate the distribution of genes functionally related to immune response and apoptosis, the two important determinants of viral virulence, in each part, the DE genes were input for GO analysis. The results showed that there were 6, 17 and 9 genes in part 2, 3 and 4, respectively, enriched to immune and innate immune response and more than two of three (23/32), such as TLR3, MYD88, FADD, PIK3, INFB, B2M, IL8 and IL15, were down-regulated in virulent SCK2 infected kidney cells (Fig. 5B and C). There were 2, 24 and 7 genes in part 1, 4 and 5, respectively, enriched to apoptotic processes and most of them (31/33) were up-regulated in virulent SCK2 infected kidney cells (Fig. 5B and D). In addition, genes encoding metabolic pathways, such as the metabolism of amino acids, fatty acid, carbon, drugs and other substances, were enriched in part 1–3 and down-regulated differentially in very virulent SCDY2 and virulent SCK2 infected kidney cells. Genes encoding oxidative phosphorylation, glycerophospholipid metabolism, phosphatidylinositol signaling system, ubiquitin mediated proteolysis, herpes simplex infection and nitrogen metabolism were enriched in part 5 and up-

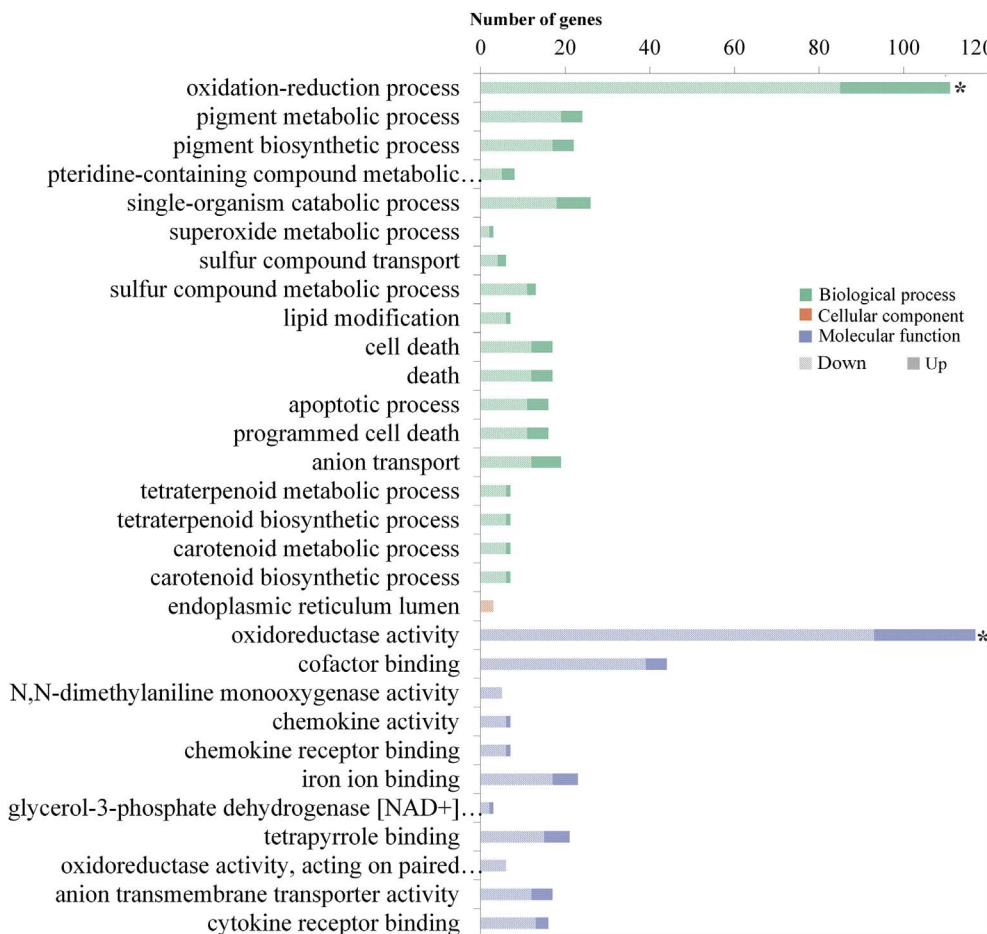


Fig. 3. GO analysis of differential expression genes. DE genes of SCDY2 infected group were categorized into the three main GO categories including biological process, cellular component and molecular function. (*) represents significantly enriched functions.

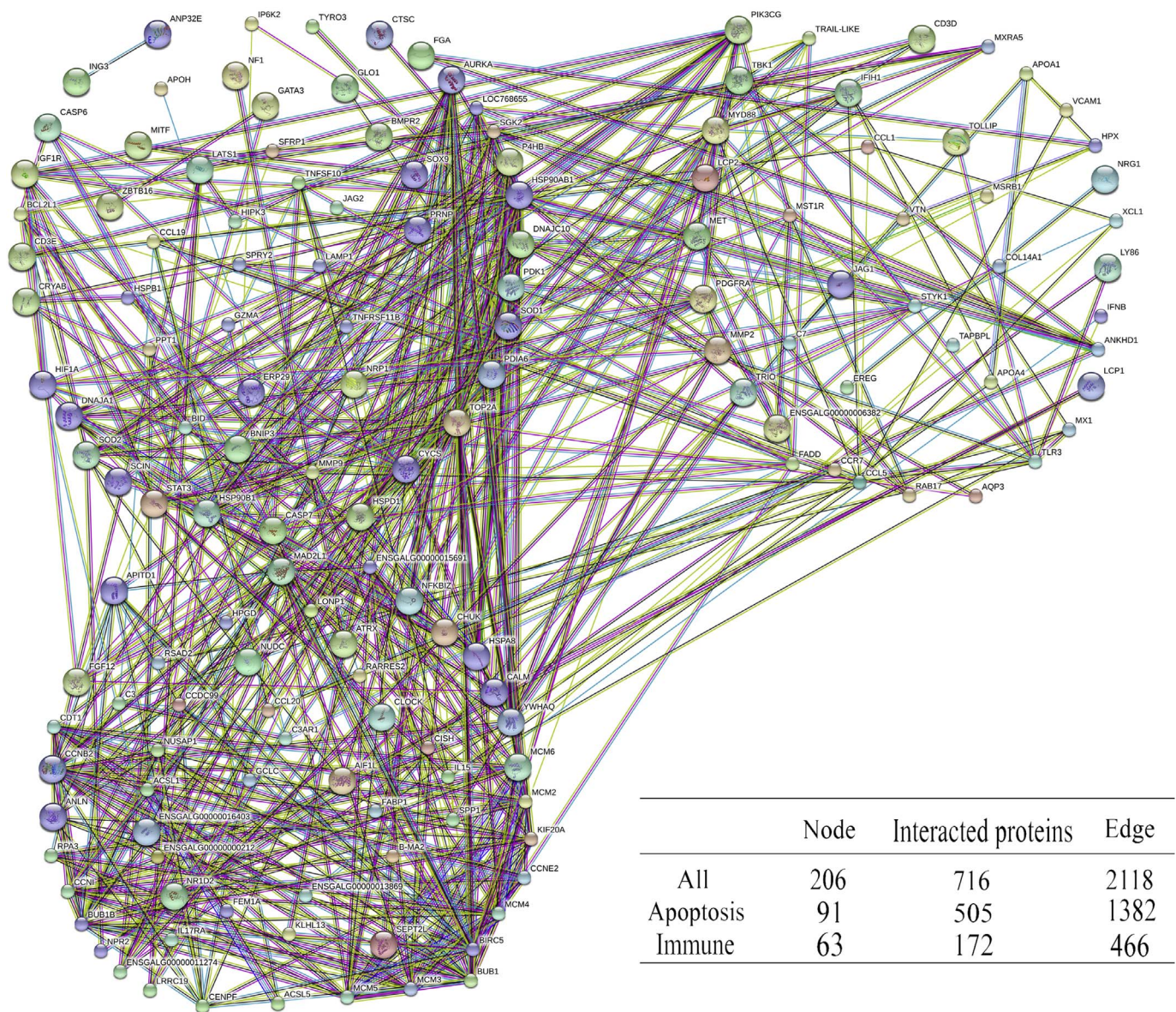


Fig. 4. PPI network constructed with DE genes in very virulent SCDY2. The disconnected nodes were hidden in the network and the data on the two main clusters were shown in the right bottom.

regulated differentially in SCDY2 and SCK2 infected kidney cells. These data suggested that activation of apoptosis and suppression of innate immune response occurred in very virulent SCDY2 infected kidney cells at 5 dpi and did partially in virulent SCK2 infected kidney cells.

3.4. Apoptosis in virulent virus infected kidney cells

The above data on genome-wide analysis of gene expression post IBV infection displayed that virulent nephropathogenic IBV may induce apoptosis in chicken kidney cells. To address the tissue, apoptosis in virulence different IBV inoculated kidney cells was studied experimentally. The ratio of Bax/Bcl2 expression level increased after virulent IBV infection and consistent with the virulence determined previously by experiment in chicken. The ratio for LDT3-A inoculated group was slightly lower ($p > 0.05$) than that of mock inoculated group; and those for the three viruses, SCDY2, SCK2 and LDT3-A, inoculated groups were significantly ($p < 0.05$ or $p < 0.01$) different from each other and ranged from low to high while viral virulence enhanced (Fig. 6 A).

To demonstrate apoptosis taken place in virulent nephropathogenic

IBV infected kidney cells, kidney tissue of the four experimental groups was sectioned and stained to detect apoptosis by TUNEL fluorescent assay. The apoptotic cells in the sections of each group were counted and the results exhibited that the number of apoptotic cells in SCDY2 infected group were the highest among all the groups and significantly ($p < 0.01$) different from the others, and the number of apoptotic cells in SCK2 infected group were also different significantly ($p < 0.05$) from the LDT3-A and mock infected groups (Fig. 6B). The FITC-labeled apoptotic cells in the representative pictures of each group were showed in Fig. 6C. Combined the above experimental data together, it could be concluded that post inoculation of nephropathogenic IBVs of different virulence, apoptosis occurred differentially in chicken kidney cells, positively correlated to the virulence of the virus applied.

4. Discussion

4.1. Induction of apoptosis in virulent nephropathogenic IBV infected kidney cells

In the present study, regulation of gene expression in chicken kidney

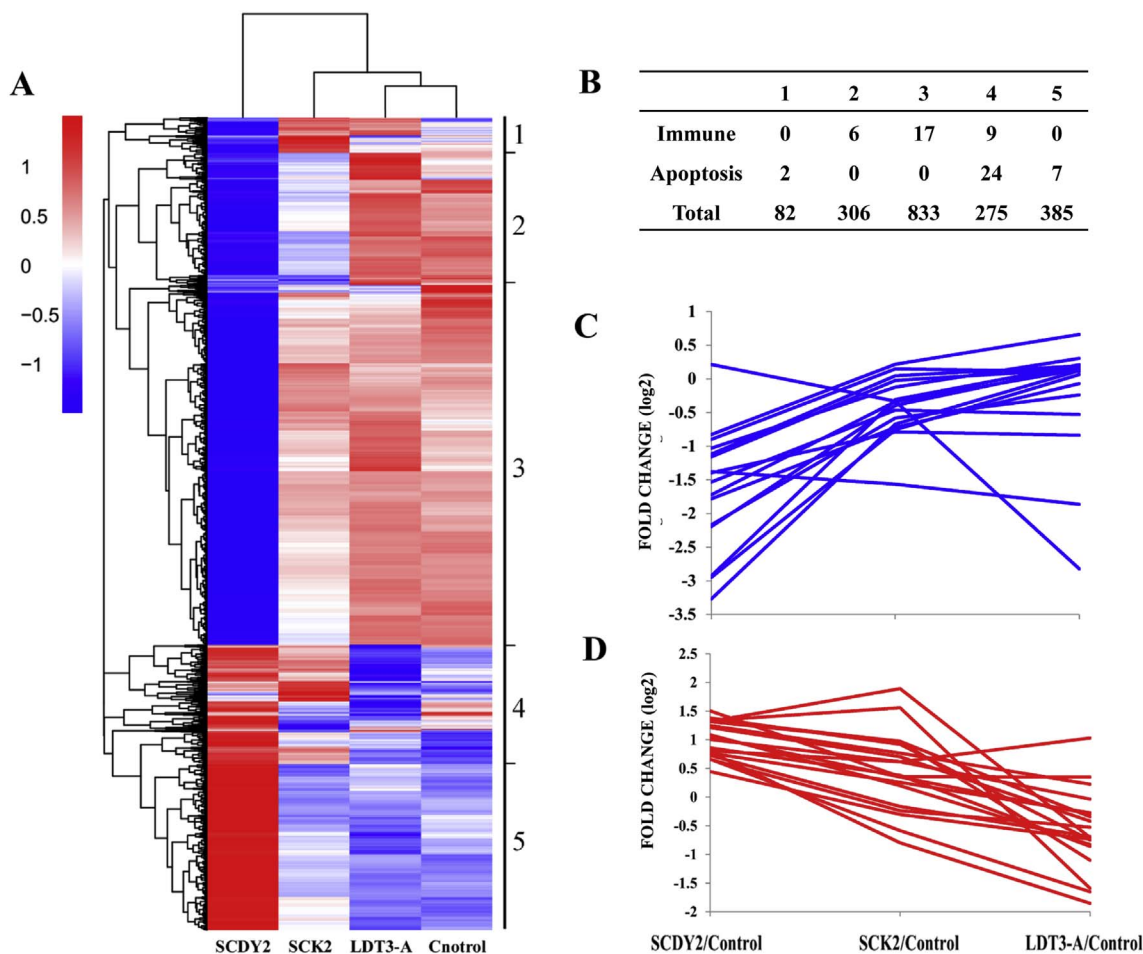


Fig. 5. Clustering analysis of DE genes in kidney cells inoculated different IBV strains. (A) Hierarchical clustering map of DE genes among the four experimental groups were classified into five parts according to gene expression pattern. (B) DE genes functionally related to immune response and apoptosis determined by GO analysis were extracted from each five part of Fig. 5 A and listed with the number of total DE genes in each part from 1 to 5. Gene expression profiles on immune response (C) and apoptosis (D) across the three virus inoculated groups were reconstructed by using the data extracted from part 3 (C) and 4 (D) of Fig. 5 A, respectively.

cells infected with nephropathogenic IBV was analyzed. Chicks inoculated virulent strains such as SCDY2 and SCK2 exhibited severe clinical signs and renal lesions as reported previously [12,34,35] and also resulted in modification of gene expression and activation of apoptosis in kidney cells. However, apoptosis induced by the two viral strains is quite different. The very virulent SCDY2 induced apoptosis in kidney cells was characterized as 1.) more genes functionally related to apoptotic processes were significantly up-regulated (Fig. 5 D); 2.) metabolic stress in these cells was high as shown in GO, KEGG and clustering analysis; and 3.) more cells in the kidney became apoptotic (Fig. 6B and C). The present experimental data suggested that the pathogenicity of virulent nephropathogenic IBV might be largely related to the ability to induce apoptosis in kidney cells.

Recently, apoptosis in chicken embryo kidney cells and tracheal epithelial cells were detected during the infection of virulent IBVs [36]. The present study demonstrated that a group of genes involved in apoptosis were differentially regulated in chicken kidney cells while infected with IBVs of different virulence, and the intrinsic and extrinsic pathways were the main approaches to apoptosis in these cells. Interestingly, the same apoptotic pathways were detected in chicken macrophage DH11 cells [37] and endoplasmic reticulum stress was reported as apoptotic pathways in mammal vero cells when both were infected with IBV Beaudette strain [38], indicating the approach to apoptosis in chicken is different from those in mammalian Vero cells.

4.2. Suppression of innate immune response in virulent IBV infected kidney cells

Innate immune response is one of the most important factors to constrict virus spreading and replication in the initial stage of infection. TLR3 signaling pathway in SCDY2 infected kidney cells seemed to be suppressed for several genes in the signaling pathway, such as TLR3, MYD88, FADD, PIK3 and IFN-β, were down-regulated. The expression profiles of TLR3 and IFN-β were consistent with other two reports by Chhabra et al. [36] and Okino et al. [39]. Okino et al. further indicated that down-regulation of TLR7 associated with severe renal lesion and an enhanced capability of replication of virulent IBV isolate post challenge [39]. The present study suggested that innate immune response was repressed at least partially in kidney cells challenged by virulent nephropathogenic IBV and the suppression might be positively related to the virulence of the viruses since expression of the relevant genes in SCK2 group was less suppressed than those in very virulent SCDY2 inoculated group (Fig. 5C).

Suppression of innate immune response by infection of virulent nephropathogenic IBV would decrease the restriction to viral replication in these cells, which may trigger and enhance the induction of apoptosis by productive viral replication in turn. In this way, suppression of innate immune response in kidney cells might be a pathogenic determinant for virulent nephropathogenic IBV.

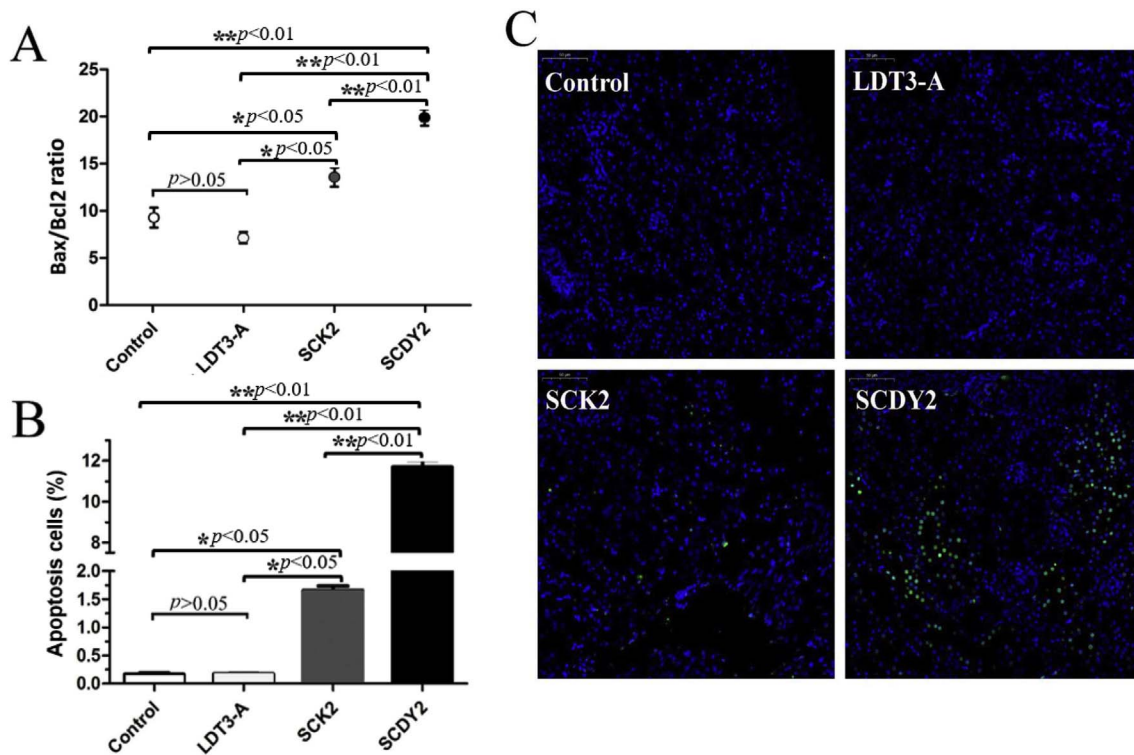


Fig. 6. Induction of apoptosis in kidney cells post virulent IBV infection. (A) The ratio of Bax/Bcl2 detected in kidney cells inoculated with SCDY2, SCK2, LDT-3 and mock at 5 dpi. (B) Apoptotic cells in kidney inoculated or mock inoculated IBV were counted at 5 dpi. (C) The representative pictures of kidney cells infected or mock infected with IBV stained by TUNEL fluorescent assay at 5 dpi show the apoptotic cells in kidney (green cells). (For interpretation of the references to colour in this figure legend, the reader is referred to the web version of this article.)

4.3. Reproduction of virulent nephropathogenic IBV in kidney cells

The IBV strains used in the study are nephropathogenic and replicate in tubules and ducts, causing nephritis while inoculation to SPF chicken [1,40]. The present results showed that replication of nephropathogenic IBV in kidney cells is positively related to the virulence of the virus. The highest, high and low viral copy number were detected in the group infected with very virulent SCDY2, virulent SCK2 and non-virulent LDT3-A, respectively (Fig. 1A and E). These virus replication data indicated that the more virulent the virus, the more efficient the virus replication in kidney cells.

Efficient replication of IBVs in kidney cells depends on viral tropism, intrinsic ability of virus replication in cells and intracellular environment for virus replication. S1 glycoprotein plays a major role in viral tissue tropism and hence partly determines viral virulence [7,41]. Viral replicase gene of avian IBV may affect viral replication and also reported to be a determinant of pathogenicity [42]. Present study demonstrated that innate immune response was down-regulated in very virulent SCDY2 infected kidney cells, which might disarm at least partially the host's restriction to virus and build up a favorable intracellular environment for viral propagation. The process of developing live and attenuated vaccine also indicated that alternation of virulent nephropathogenic IBV into non-virulent vaccine strain, such as K2p170 [43] and LDT3-A [33], by repeated passing in embryonated chicken eggs was accompanied with narrow of their tropism to respiratory tract and restriction of their replication in kidney cells.

In addition, cell apoptosis may also promote replication and spread of the virus as reported in Dengue virus-2 [44] and PRRSV [45], since the number of apoptotic cells in kidney post nephropathogenic IBV infection were positively related to the viral titer reached in these cells.

4.4. Virus and host encoded sequences involved induction of apoptosis

Induction of apoptosis by virus infection has been investigated in several species of coronavirus. Overexpression of virus encoded sequences such as 3a [46], 3b [47] and 7a [48] of SARS coronavirus were demonstrated to induce apoptosis. In the present study, a massive viral RNA of 3a, 3b and E in very virulent SCDY2 inoculated kidney cells, as well as in the virulent SCK2 inoculated were detected positively related to their virulence (Fig. 1A). Hong SM et al. reported that 3a, 3b and 5b of IBV might inhibit innate immunity and play a role in host adaptation and evasion of host immune response [6]. However, it is possible that these sequences also take part in the process of induction of apoptosis directly in kidney cells during virulent IBV infection.

Another group of molecules that may promote apoptosis in kidney cells while IBV infection were the host encoded siRNAs. A research carried out by the same group on regulation of IBV replication by host encoded siRNAs in chicken kidney cells indicated that some host genes related to innate immune response such as TLR3 and MYD88 were negatively regulated by host encoded siRNAs [49], indicating the molecules direct regulation of host cells into apoptosis post virulent IBV infection is more complicated and largely unknown at present.

In conclusion, infection of virulent nephropathogenic IBV modified a number of gene expression in kidney cells. The up-regulation of apoptosis pathway and down-regulation of genes on innate immune response and cell metabolism were observed in comparative transcriptome analysis and positively correlated to the virulence of the virus inoculated. In addition, increased viral reproductive replication and cell apoptosis were detected in very virulent SCDY2 inoculated group. These data indicated that induction of apoptosis in kidney cells may be a key pathogenic determinant and associated with the virulence of nephropathogenic IBV.

Compliance with ethical standards

Conflict of interest

All authors declare that they have no conflict of interest.

Ethical approval

All animal studies are approved by the Animal Ethics Committee of Sichuan University. All authors have seen the manuscript and approved to submit to “Microbial Pathogenesis”.

Acknowledgment

This research was supported by the National Key R&D Program of China (2017YFD0500703), State Natural Sciences Foundation (31302094, 31372442), the Program of Main Livestock Standardized Breeding Technology Research and Demonstration (2016NYZ0052), the Project for Science and Technology Support Program of Sichuan Province (2014NZ0002, 2016NZ0003) and the China Agriculture Research System (CARS-40) National System for Layer Production Technology (CARS-40-K14).

Appendix A. Supplementary data

Supplementary data related to this article can be found at <http://dx.doi.org/10.1016/j.micpath.2017.11.031>.

References

- [1] D. Cavanagh, Coronavirus avian infectious bronchitis virus, *Veterinary Res.* 38 (2007) 281–297.
- [2] V.R. Reddy, S. Theuns, I.D. Roukaerts, M. Zeller, J. Matthijssens, H.J. Nauwynck, Genetic characterization of the Belgian nephropathogenic infectious bronchitis virus (NIBV) reference strain B1648, *Viruses* 7 (2015) 4488–4506.
- [3] M.L. Mo, M. Li, B.C. Huang, W.S. Fan, P. Wei, T.C. Wei, et al., Molecular characterization of major structural protein genes of avian coronavirus infectious bronchitis virus isolates in southern China, *Viruses* 5 (2013) 3007–3020.
- [4] W. Zhang, K.M. Bouwman, S.J. van Beurden, S.R. Ordonez, M. van Eijk, H.P. Haagsman, et al., Chicken mannose binding lectin has antiviral activity towards infectious bronchitis virus, *Virology* 509 (2017) 252–259.
- [5] M.L. Mo, S.M. Hong, H.J. Kwon, I.H. Kim, C.S. Song, J.H. Kim, Genetic diversity of spike, 3a, 3b and e genes of infectious bronchitis viruses and emergence of new recombinants in Korea, *Viruses* 5 (2013) 550–567.
- [6] S.M. Hong, H.J. Kwon, I.H. Kim, M.L. Mo, J.H. Kim, Comparative genomics of Korean infectious bronchitis viruses (IBVs) and an animal model to evaluate pathogenicity of IBVs to the reproductive organs, *Viruses* 4 (2012) 2670–2683.
- [7] F. Bande, S.S. Arshad, A.R. Omar, M.H. Bejo, M.S. Abubakar, Y. Abba, Pathogenesis and diagnostic approaches of avian infectious bronchitis, *Adv. Virol.* 2016 (2016) 4621659.
- [8] Z. Zhang, Y. Zhou, H. Wang, F. Zeng, X. Yang, Y. Zhang, et al., Molecular detection and Smoothing spline clustering of the IBV strains detected in China during 2011–2012, *Virus Res.* 211 (2016) 145–150.
- [9] F. Awad, R. Chhabra, M. Baylis, K. Ganapathy, An overview of infectious bronchitis virus in chickens, *Worlds Poult. Sci. J.* 70 (2014) 375–384.
- [10] R. Zhao, J. Sun, T. Qi, W. Zhao, Z. Han, X. Yang, et al., Recombinant Newcastle disease virus expressing the infectious bronchitis virus S1 gene protects chickens against Newcastle disease virus and infectious bronchitis virus challenge, *Vaccine* 35 (2017) 2435–2442.
- [11] B. Jordan, Vaccination against infectious bronchitis virus: a continuous challenge, *Vet. Microbiol.* 206 (2017) 137–143.
- [12] D.E. Swayne, J.R. Glisson, L.R. McDougald, L.K. Nolan, D.L. Suarez, V.L. Nair, *Diseases of Poultry*, thirteenth ed., (2013) *Diseases of Poultry*.
- [13] W.Q. Fan, H.N. Wang, Y. Zhang, Z.B. Guan, T. Wang, C.W. Xu, et al., Comparative dynamic distribution of avian infectious bronchitis virus M41, H120, and SAIBK strains by quantitative real-time RT-PCR in SPF chickens, *Biosci. Biotechnol. Biochem.* 76 (2012) 2255–2260.
- [14] Z. Cao, Z. Han, Y. Shao, X. Liu, J. Sun, D. Yu, et al., Proteomics analysis of differentially expressed proteins in chicken trachea and kidney after infection with the highly virulent and attenuated coronavirus infectious bronchitis virus in vivo, *Proteome Sci.* 10 (2012) 24.
- [15] F. Cong, X. Liu, Z. Han, Y. Shao, X. Kong, S. Liu, Transcriptome analysis of chicken kidney tissues following coronavirus avian infectious bronchitis virus infection, *BMC Genomics* 14 (2013) 743.
- [16] A. Dar, S. Munir, S. Vishwanathan, A. Manuja, P. Griebel, S. Tikoo, et al., Transcriptional analysis of avian embryonic tissues following infection with avian infectious bronchitis virus, *Virus Res.* 110 (2005) 41–55.
- [17] X. Lin, R. Wang, J. Zhang, X. Sun, Z. Zou, S. Wang, et al., Insights into human astrocyte response to H5N1 infection by microarray analysis, *Viruses* 7 (2015) 2618–2640.
- [18] K. Leskinen, B.G. Blasdel, R. Lavigne, M. Skurnik, RNA-sequencing reveals the progression of phage-host interactions between phiR1-37 and *Yersinia enterocolitica*, *Viruses* 8 (2016) 111.
- [19] H. Yanagisawa, R. Tomita, K. Katsu, T. Uehara, G. Atsumi, C. Tateda, et al., Combined DECS analysis and next-generation sequencing enable efficient detection of novel plant RNA viruses, *Viruses* 8 (2016) 70.
- [20] J. Villacreses, M. Rojas-Herrera, C. Sanchez, N. Hewstone, S.F. Undurraga, J.F. Alzate, et al., Deep sequencing reveals the complete genome and evidence for transcriptional activity of the first virus-like sequences identified in *Aristolochia chilensis* (Maqui Berry), *Viruses* 7 (2015) 1685–1699.
- [21] X. Wang, A.J. Rosa, H.N. Oliverira, G.J. Rosa, X. Guo, M. Travnicek, et al., Transcriptome of local innate and adaptive immunity during early phase of infectious bronchitis viral infection, *Viral Immunol.* 19 (2006) 768–774.
- [22] E. Hamzic, R.B. Kjaerup, N. Mach, G. Minozzi, F. Strozzi, V. Gualdi, et al., RNA sequencing-based analysis of the spleen transcriptome following infectious bronchitis virus infection of chickens selected for different mannose-binding lectin serum concentrations, *BMC genomics* 17 (2016) 82.
- [23] Y. Zhong, Y.W. Tan, D.X. Liu, Recent progress in studies of arterivirus- and coronavirus-host interactions, *Viruses* 4 (2012) 980–1010.
- [24] H.D. Mitchell, A.J. Einfeld, A.C. Sims, J.E. McDermott, M.M. Matzke, B.J. Webb-Robertson, et al., A network integration approach to predict conserved regulators related to pathogenicity of influenza and SARS-CoV respiratory viruses, *PLoS One* 8 (2013) e69374.
- [25] N. Irigoyen, A.E. Firth, J.D. Jones, B.Y. Chung, S.G. Siddell, I. Brierley, High-resolution analysis of coronavirus gene expression by RNA sequencing and ribosome profiling, *PLoS Pathog.* 12 (2016) e1005473.
- [26] C. Liu, H.Y. Xu, D.X. Liu, Induction of caspase-dependent apoptosis in cultured cells by the avian coronavirus infectious bronchitis virus, *J. Virol.* 75 (2001) 6402–6409.
- [27] Y. Zhong, Y. Liao, S. Fang, J.P. Tam, D.X. Liu, Up-regulation of Mcl-1 and Bak by coronavirus infection of human, avian and animal cells modulates apoptosis and viral replication, *PLoS One* 7 (2012) e30191.
- [28] Y. Liao, T.S. Fung, M. Huang, S.G. Fang, Y. Zhong, D.X. Liu, Upregulation of CHOP/GADD153 during coronavirus infectious bronchitis virus infection modulates apoptosis by restricting activation of the extracellular signal-regulated kinase pathway, *J. Virol.* 87 (2013) 8124–8134.
- [29] A.M. Kameka, S. Haddadi, D.S. Kim, S.C. Cork, M.F. Abdul-Careem, Induction of innate immune response following infectious bronchitis corona virus infection in the respiratory tract of chickens, *Virology* 450–451 (2014) 114–121.
- [30] H.J. Ramos, J. Michael Gale, RIG-I-like receptors and their signaling crosstalk in the regulation of antiviral immunity, *Curr. Opin. Virol.* 1 (2011) 167.
- [31] L. Sun, S. Liu, Z.J. Chen, SnapShot: pathways of antiviral innate immunity, *Cell* 140 (2010) 436–e2.
- [32] X. Wu, X. Yang, P. Xu, L. Zhou, Z. Zhang, H. Wang, Genome sequence and origin analyses of the recombinant novel IBV virulent isolate SAIBK2, *Virus Genes* (2016) 509–520.
- [33] Z. Han, T. Zhang, Q. Xu, M. Gao, Y. Chen, Q. Wang, et al., Altered pathogenicity of a t/CH/LDT3/03 genotype infectious bronchitis coronavirus due to natural recombination in the 5′-17kb region of the genome, *Virus Res.* 213 (2016) 140–148.
- [34] B.Y. Chen, C. Itakura, Cytopathology of chick renal epithelial cells experimentally infected with avian infectious bronchitis virus, *Avian Pathol.* 25 (1996) 675–690.
- [35] S. Yan, X. Liu, J. Zhao, G. Xu, Y. Zhao, G. Zhang, Analysis of antigenicity and pathogenicity reveals major differences among QX-like infectious bronchitis viruses and other serotypes, *Vet. Microbiol.* 203 (2017) 167–173.
- [36] R. Chhabra, S.V. Kuchipudi, J. Chantrey, K. Ganapathy, Pathogenicity and tissue tropism of infectious bronchitis virus is associated with elevated apoptosis and innate immune responses, *Virology* 488 (2016) 232–241.
- [37] X. Han, Y. Tian, R. Guan, W. Gao, X. Yang, L. Zhou, et al., Infectious bronchitis virus infection induces apoptosis during replication in chicken macrophage HD11 cells, *Viruses* 9 (2017) 198.
- [38] T.S. Fung, L. Ying, X.L. Ding, The endoplasmic reticulum stress sensor IRE1 α protects cells from apoptosis induced by the coronavirus infectious bronchitis virus, *J. Virol.* 88 (2014) 12752.
- [39] C.H. Okino, M.A. Mores, I.M. Trevisol, A. Coldebella, H.J. Montassier, L. Brentano, Early immune responses and development of pathogenesis of avian infectious bronchitis viruses with different virulence profiles, *PLoS one* 12 (2017) e0172275.
- [40] Q. Huang, X. Gao, P. Liu, H. Lin, W. Liu, G. Liu, et al., The relationship between liver-kidney impairment and viral load after nephropathogenic infectious bronchitis virus infection in embryonic chickens, *Poult. Sci.* 96 (2017) 1589–1597.
- [41] Z. Zhang, X. Yang, P. Xu, X. Wu, L. Zhou, H. Wang, Heat shock protein 70 in lung and kidney of specific-pathogen-free chickens is a receptor-associated protein that interacts with the binding domain of the spike protein of infectious bronchitis virus, *Arch. Virol.* 162 (2017) 1625–1631.
- [42] M. Armesto, D. Cavanagh, P. Britton, The replicase gene of avian coronavirus infectious bronchitis virus is a determinant of pathogenicity, *Plos One* 4 (2009) e7384.
- [43] H.J. Lee, H.N. Youn, J.S. Kwon, Y.J. Lee, J.H. Kim, J.B. Lee, et al., Characterization of a novel live attenuated infectious bronchitis virus vaccine candidate derived from a Korean nephropathogenic strain, *Vaccine* 28 (2010) 2887–2894.
- [44] Y.R. Lee, H.Y. Lei, M.T. Liu, J.R. Wang, S.H. Chen, Y.F. Jiang-Shieh, et al., Autophagic machinery activated by dengue virus enhances virus replication, *Virology* 374 (2008) 240–248.
- [45] M. Ge, Y. Zhang, Y. Liu, T. Liu, F. Zeng, Propagation of field highly pathogenic

- porcine reproductive and respiratory syndrome virus in MARC-145 cells is promoted by cell apoptosis, *Virus Res.* 213 (2016) 322–331.
- [46] C.M. Chan, H. Tsoi, W.M. Chan, S. Zhai, C.O. Wong, X. Yao, et al., The ion channel activity of the SARS-coronavirus 3a protein is linked to its pro-apoptotic function, *Int. J. Biochem. Cell Biol.* 41 (2009) 2232–2239.
- [47] S. Khan, B.C. Fielding, T.H. Tan, C.F. Chou, S. Shen, S.G. Lim, et al., Over-expression of severe acute respiratory syndrome coronavirus 3b protein induces both apoptosis and necrosis in Vero E6 cells, *Virus Res.* 122 (2006) 20–27.
- [48] Y.X. Tan, T.H.P. Tan, M.J.R. Lee, P.Y. Tham, V. Gunalan, J. Druce, et al., Induction of apoptosis by the severe acute respiratory syndrome coronavirus 7a protein is dependent on its interaction with the Bcl-XL protein, *J. Virol.* 81 (2007) 6346–6355.
- [49] X. Yang, W. Gao, H. Liu, J. Li, D. Chen, F. Yuan, Z. Zhang, H. Wang, MicroRNA transcriptome analysis in chicken kidneys in response to differing virulent infectious bronchitis virus infections, *Arch. Virol.* (2017) 1–9.